Journal of Organometallic Chemistry 693 (2008) 2641–2644

Contents lists available at ScienceDirect

Journal of Organometallic Chemistry

journal homepage: www.elsevier.com/locate/jorganchem

Note

Reaction of $[M(CO)_4]^-$ (M = Ir, Rh) with cyclopropenyl tetrafluoroborate – Ring opening and coupling of cyclopropenyl ligands to form dinuclear metal complexes

Pek Ke Chan, Weng Kee Leong *

Department of Chemistry, National University of Singapore, Kent Ridge, Singapore 117543, Singapore

ARTICLE INFO

Article history:
Received 13 March 2008
Received in revised form 28 April 2008
Accepted 28 April 2008
Available online 6 May 2008

Keywords:
Diiridium
Cyclopropenyl
Ring opening
C–C coupling

ABSTRACT

Reaction of the iridium tetracarbonylate [PPN][$Ir(CO)_4$] (**1a**) with triphenylcyclopropenyl tetrafluoroborate [C_3Ph_3][BF_4] afforded two dinuclear species $Ir_2(CO)_4(\mu,\eta^1{:}\eta^2\text{-}C_3Ph_3)(\mu,\eta^2{:}\eta^3\text{-}C_3Ph_3)$ (**2**) and $Ir_2(CO)_4(\mu,\eta^4{:}\eta^4\text{-}C_6Ph_6)$ (**3a**) resulting from the ring opening and in the latter case, coupling of the resulting acyclic, propenyl ligands. The analogous reaction with [PPN][$Rh(CO)_4$] (**1b**) afforded only the rhodium analogue for **3a**.

1. Introduction

The simplest cyclic enyl ligand, η^3-cyclopropenyl, can undergo $\eta^1 \rightarrow \eta^3$ ring-slippage in a similar fashion to its acylic η^3-propenyl (allyl) analogue [1]. Our interest in this class of compound was prompted by our earlier finding that the photolysis of a cyclohexane solution of $Cp^*Ir(CO)_2$ under a CO atmosphere produced small amounts of cyclohexanecarboxaldehyde [2]. We surmised that the low yield may be related to the fact that migratory insertion of CO is less favourable for Ir than for Rh, but this may be encouraged by steric effects [3]. We were thus interested in extending our study to cyclopropenyltricarbonyliridium with the view that it may be possible to create greater steric crowding around the metal centre through the incorporation of a larger number of ligands. Compounds such as those shown in Chart 1 can be synthesized via the reaction of cyclopropenyl cation or halide with anionic or neutral metal complexes [4–6], although ring opening reactions with some transition metal complexes are also known; a common product is the η^3-oxycyclobutenyl complex which may be formed via CO insertion [7].

In our attempt at the synthesis of the η^3-triphenylcyclopropenyltricarbonyl iridium complex $(C_3Ph_3)Ir(CO)_3$ via an ionic coupling reaction between the carbonylate [PPN][$Ir(CO)_4$] (**1a**) and triphenylcyclopropenyl tetrafluoroborate [C_3Ph_3][BF_4], a reaction which is analogous to that previously reported for the preparation of $[(\eta^3\text{-}C_3{}^tBu_3)Ir(CO)_3]$ [5], we obtained instead two diiridium species $Ir_2(CO)_4(\mu,\eta^1{:}\eta^2\text{-}C_3Ph_3)(\mu,\eta^2{:}\eta^3\text{-}C_3Ph_3)$ (**2**) and $Ir_2(CO)_4(\mu,\eta^4{:}\eta^4\text{-}C_6Ph_6)$ (**3a**) (Scheme 1). A similar reaction with [PPN][$Rh(CO)_4$] (**1b**) afforded only the rhodium analogue of **3a**, *viz.*, $Rh_2(CO)_4(\mu,\eta^4{:}\eta^4\text{-}C_6Ph_6)$ (**3b**).

Ring opening of the cyclopropenyl ring in all three products has been confirmed by the molecular structures as determined by single crystal X-ray diffraction studies; the ORTEP plots of **2** and **3a** are given in Figs. 1 and 2, respectively, and selected bond parameters together with a common atomic numbering scheme for **3a** and **3b** are given in Table 1.

The two propenyl ligands in **2**, both of which bridge the Ir–Ir bond, are not the same. For one of the propenyl ligands, there is a clear difference in the C–C bond lengths (C1–C2 = 1.334(10) Å and C2–C3 = 1.504(9) Å, which are characteristic of double and sp^2–sp^3 C–C single bonds, respectively [8]) and while one terminal carbon (C3) has bonding interaction with both the iridium atoms, the other (C1) has bonding interaction with only one. In contrast, there is no distinct difference in the Ir1–C or C–C bond lengths for the other propenyl ligand (C4–C5 = 1.423(9) Å and C5–C6 = 1.443(9) Å), which are intermediate between that of a single and a double bond. The bonding modes for the ligands are thus best described as $\mu,\eta^1{:}\eta^2$ and $\mu,\eta^2{:}\eta^3$, respectively.

Compounds **3a** and **3b** are isomorphic and isostructural, and the molecules of both have a crystallographic C_2 symmetry axis passing through the midpoint of the metal–metal bond and the two central carbon atoms of the C_6 chain in the C_6Ph_6 ligand. Indeed, the difference between the metal–metal bond lengths is not statistically significant. The hydrocarbon ligand acts as a 8-electron donor and adopts a $\mu,\eta^4{:}\eta^4$ bonding mode, and is clearly the result of ring opening and coupling of two cyclopropenyls.

* Corresponding author.
E-mail address: chmlwk@nus.edu.sg (W.K. Leong).

0022-328X/$ - see front matter © 2008 Elsevier B.V. All rights reserved.
doi:10.1016/j.jorganchem.2008.04.040

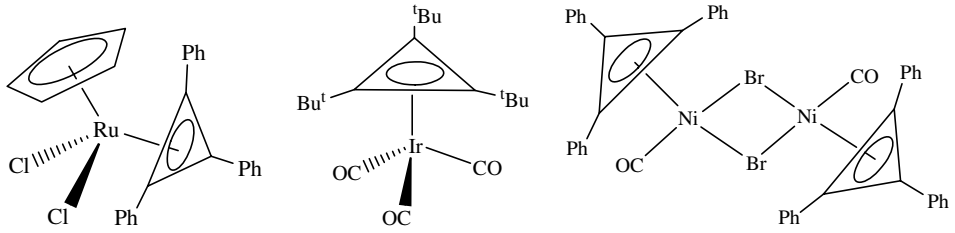

Chart 1.

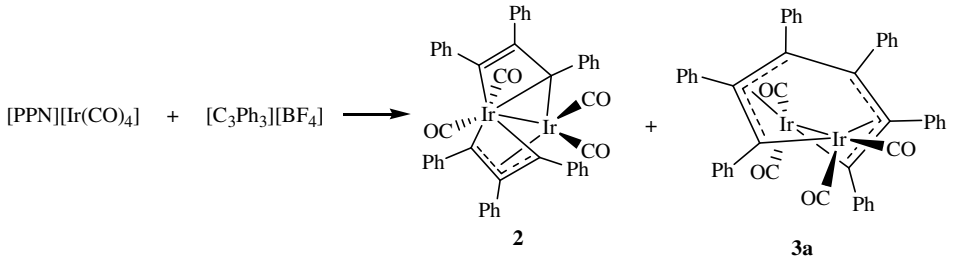

Scheme 1.

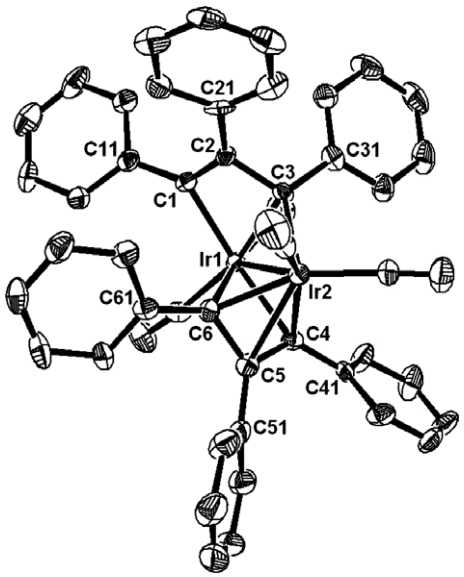

Fig. 1. ORTEP plot and selected bond lengths (Å) and angles (°) for **2**. Thermal ellipsoids are drawn at 50% probability level. Hydrogen atoms have been omitted for clarity. Ir1–Ir2 = 2.6926(4); Ir1–C1 = 2.132(6); Ir1–C3 = 2.136(7); Ir1–C4 = 2.204(6); Ir1–C6 = 2.179(7); Ir2–C3 = 2.113(6); Ir2–C4 = 2.156(7); Ir2–C5 = 2.327(7); Ir2–C6 = 2.120(7); C1–C2 = 1.334(10); C2–C3 = 1.504(9); C4–C5 = 1.423(9); C5–C6 = 1.443(9); C1–Ir1–C6 = 90.2(2); C1–Ir1–Ir2 = 94.85(18); C6–Ir1–Ir2 = 50.29(16); C3–Ir2–C4 = 96.8(2); C2–C1–Ir1 = 99.5(4); C1–C2–C3 = 101.8(6); C2–C3–Ir2 = 114.6(4); C5–C4–Ir2 = 78.1(4); C4–C5–C6 = 102.9(6).

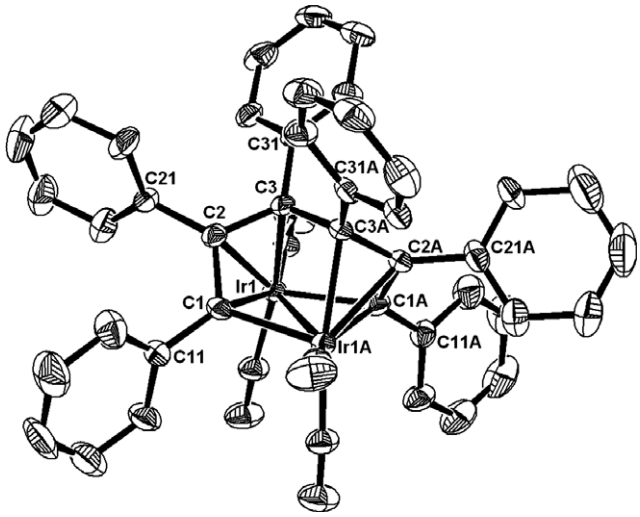

Fig. 2. ORTEP plot of **3a**. Thermal ellipsoids are drawn at 50% probability level. Hydrogen atoms have been omitted for clarity.

An attempt at preventing cleavage of the cyclopropenyl ring by slowly warming up the reaction mixture from a lower temperature was unsuccessful; essentially the same products were obtained. An attempt to dislodge the coupled ligand from **3a** by heating under a CO atmosphere also failed to afford any detectable organic species in the GC–MS analysis of the product mixture; no conversion to **2** was observed. The reverse conversion, from **2** to **3a**, also appears not to proceed; heating a toluene solution of **2** under argon at 60 °C for 5 h afforded as yet unidentified products but no **3a**.

Although cyclopropenyl ring opening is known [7], the formation of dinuclear complexes such as **2** and **3** has not been reported. The formation of compound **2** may involve initial binding of the cyclopropenyl ring to the Ir centre via a η^1-coordination mode. The subsequent loss of two CO ligands followed by bridging by the ring-opened cyclopropenyl ligands across two iridium centres would result in **2** and/or **3**. Precedence for this pathway has been reported for the rhenium complex $Re(CO)_5(\eta^1\text{-}C_3Ph_3)$, where the initially η^1-bonded cyclopropenyl ligand underwent ring opening upon UV irradiation, or by refluxing in hexane, to form a metallacycle $Re(CO)_4(C_3Ph_3)$ [9]. Nevertheless, it is not clear why dinuclear species containing a metal–metal bond are observed in our case, in contrast to the monomeric species reported by others [9,10].

2. Experimental

2.1. General procedures

All manipulations of air-sensitive materials were carried out using standard Schlenk techniques under an atmosphere of argon. Solvents were purified, dried, distilled, and stored under argon

Table 1
Common atomic numbering scheme and selected bond parameters for **3a** and **3b**

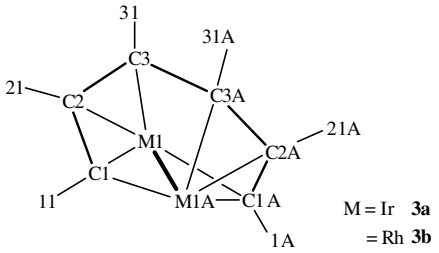

Bond distances (Å)	3a	3b	Bond angles (°)	3a	3b
M1–C1	2.144(7)	2.098(3)			
M1–C2	2.246(6)	2.237(3)	C1–M1–M1A	50.8(2)	52.30(7)
M1–C3	2.176(6)	2.172(2)	C2–C1–M1	75.0(4)	76.4(2)
M1–C1A	2.136(7)	2.180(3)	C1–C2–C3	110.6(5)	111.0(2)
M1–M1A	2.6974(5)	2.6963(4)	C2–C3–C3A	114.9(6)	115.3(2)
C1–C2	1.424(9)	1.415(3)	C1A–M1–M1A	51.1(2)	49.59(7)
C2–C3	1.458(9)	1.455(4)			
C3–C3A	1.54(1)	1.529(5)			

prior to use. TLC separations were carried out on plates coated with silica gel 60 F_{254} of 0.25 mm thickness. NMR spectra were measured on a Bruker 300 MHz FT NMR spectrometer. ^{1}H chemical shifts were referenced to residual $CHCl_3$ proton signal (δ 7.26) in $CDCl_3$. GC analyses were performed on a HP 6890 gas chromatograph equipped with a HP 5973 mass selective detector and a ZB-1 (30 m × 0.25 mm × 0.25 μm) capillary column. Mass spectra were obtained on a Finnigan MAT95XL-T spectrometer in a 3NBA matrix. Elemental analyses were carried out by the microanalytical laboratory within the department. The compounds $[C_3Ph_3][BF_4]$ (**1a**) and (**1b**) were synthesized by the literature methods [11,12].

2.2. Reaction of [PPN][Ir(CO)$_4$] (*1a*) with $[C_3Ph_3][BF_4]$

To a solution of **1a** (106.0 mg, 126 μmol) in dcm (5 ml) in a Schlenk tube was added dropwise a suspension of $[C_3Ph_3][BF_4]$ (45.0 mg, 127 μmol) in dcm (5 ml). The solution turned wine-red and darkened to deep purple within a few minutes. The solution was stirred at room temperature for 0.5 h after which the solvent was removed under reduced pressure. The resultant purple oil was extract with toluene (3 × 2 ml), leaving behind a residue which was found to contain [PPN][BF_4] (51.8 mg, 66%). The toluene extract was concentrated under reduced pressure and separated by TLC using ether:hexane (1:2, v/v) as eluent to give two major overlapping bands which could not be completely separated.

Band 1 (purple) (R_f = 0.57) afforded black crystals identified to be $Ir_2(CO)_4(\mu,\eta^1{:}\eta^2\text{-}C_3Ph_3)(\mu,\eta^2{:}\eta^3\text{-}C_3Ph_3)$, **2** (yield = 17.3 mg, 13%). IR (toluene): ν_{CO} 2059 (m), 2037 (vs), 2011 (m), 1990 (m) cm^{-1}. IR (hex): ν_{CO} 2061 (m), 2041 (vs), 2016 (m), 1996 (m) cm^{-1}. ^{1}H NMR ($CDCl_3$): δ 7.5–6.7 (m, aromatic). MS FAB$^+$ (*m*/*z*): 1030 [M]$^+$. HR-MS FAB$^+$ (*m*/*z*): Calc. for $C_{46}H_{30}O_4{}^{[191]}Ir^{[193]}Ir$: 1030.1374. Found: 1030.1381.

Band 2 (yellow) (R_f = 0.54) afforded dark red crystals identified to be $Ir_2(CO)_4(\mu,\eta^4{:}\eta^4\text{-}C_6Ph_6)$, **3a** (yield = 43.4 mg, 34%). IR (tol): ν_{CO} 2055 (s), 2030 (vs), 1990 (m), 1976 (s) cm^{-1}. IR (hex): ν_{CO} 2059 (m), 2054 (w), 2033 (vs), 1996 (w) 1990 (w), 1981 (s) cm^{-1}. ^{1}H NMR ($CDCl_3$): δ 7.5–6.7 (m, aromatic). Anal. Calc. for $C_{46}H_{30}O_4Ir_2 \cdot 1/2Et_2O$: C, 54.15; H, 3.58. Found: C, 54.02; H, 3.54%. MS FAB$^+$ (*m*/*z*): 1030 [M]$^+$. HR-MS FAB$^+$ (*m*/*z*): Calc. for $C_{46}H_{30}O_4{}^{[191]}Ir^{[193]}Ir$: 1030.1374. Found: 1030.1339. Calc. for $C_{46}H_{30}O_4{}^{[193]}Ir_2$: 1032.1397. Found: 1032.1362.

The same reaction was repeated by allowing a solution initially maintained at −78 °C to slowly warm up towards room temperature until the reaction was completed (as indicated by the disappearance of peaks in the carbonyl stretching region due to $[Ir(CO)_4]^-$). Evaporation of the solvent under reduced pressure at low temperature gave essentially the same products in similar yields.

2.3. Attempted carbonylation of *3a*

A solution of **3a** (5.0 mg, 5 μmol) in toluene/hexane (1:1, v/v) was heated at 50 °C under CO (1 atm) for 3 h. IR analysis showed only peaks due to unreacted **3a**. The mixture was further heated for 15 h at 50 °C, and for 10 h at 70 °C. GC–MS analysis of the reaction mixture did not show the presence of any organic products.

2.4. Reaction of [PPN][Rh(CO)$_4$] (*1b*) with $[C_3Ph_3][BF_4]$

A suspension of $[C_3Ph_3][BF_4]$ (45.0 mg, 127 μmol) in dcm (5 ml) was added dropwise to a solution of **1b** (90.0 mg, 119 μmol) in dcm (5 ml) in a Schlenk tube that was maintained at −78 °C in a dry ice-acetone bath. The solution was stirred and allowed to warm to room temperature during which it darkened to a wine-red colour. The solvent was removed under reduced pressure and the residue was redissolved in a minimum amount of dcm and subjected to TLC separation. Elution with dcm:hexane (1:3, v/v) as eluent afforded a red band (R_f = 0.37) of $Rh_2(CO)_4(\mu,\eta^4{:}\eta^4\text{-}C_6Ph_6)$, **3b** (yield = 49.4 mg, 49%). X-ray diffraction quality crystals of **3b** were grown from a hexane solution at 5 °C. IR (KBr): ν_{CO} 2054 (m), 2031 (vs), 2009 (s), 1995 (w) cm^{-1}. IR (hex): ν_{CO}2060 (m), 2045 (vs), 2014 (s), 2004 (w) cm^{-1}. ^{1}H NMR ($CDCl_3$): δ 7.8–6.8 (m, aromatic). Anal. Calc. for $C_{46}H_{30}O_4Rh_2$: C, 64.81; H, 3.55. Found: C, 64.83; H, 4.03%. MS FAB$^+$ (*m*/*z*): 824 [M−CO]$^+$, 796 [M−2(CO)]$^+$, 768 [M−3(CO)]$^+$, 740 [M−4(CO)]$^+$. HR-MS FAB$^+$ (*m*/*z*): Calc. for $C_{46}H_{30}O_4{}^{[103]}Rh_2$: 852.0249. Found: 852.0259.

Table 2
Crystal and refinement data for compounds **2**, **3a** and **3b**

	2	3a	3b
Empirical formula	$C_{46}H_{30}Ir_2O_4$	$C_{46}H_{30}Ir_2O_4$	$C_{46}H_{30}Rh_2O_4$
Formula weight	1031.10	1031.10	852.52
Temperature	223(2)	223(2)	223(2)
Crystal system	Triclinic	Monoclinic	Monoclinic
Space group	$P\bar{1}$	$C2/c$	$C2/c$
a (Å)	11.2098(8)	12.8167(11)	12.7410(3)
b (Å)	11.6987(8)	19.5537(18)	19.6927(4)
c (Å)	16.2944(12)	15.4177(14)	15.4404(3)
α (°)	71.4880(10)	90	90
β (°)	74.6470(10)	106.897(2)	106.5150(10)
γ (°)	65.5560(10)	90	90
Volume (Å^3)	1822.5(2)	3697.1(6)	3714.24(14)
Z	2	4	4
D_{Calc} (Mg m^{-3})	1.879	1.852	1.525
Absorption coefficient (mm^{-1})	7.339	7.236	0.932
F(000)	984	1968	1712
Crystal size (mm^3)	0.34 × 0.08 × 0.04	0.16 × 0.10 × 0.08	0.27 × 0.14 × 0.09
Reflections collected	16752	15398	19917
Independent reflections [R_{int}]	7438 [0.0347]	4689 [0.0555]	5453 [0.0449]
Maximum and minimum transmission	0.7578 and 0.1893	0.5952 and 0.3906	0.9208 and 0.7869
Data/restraints/parameters	7438/0/469	4689/0/235	5453/0/235
Goodness-of-fit on F^2	1.020	1.059	1.085
Final *R* indices [$9i > 2\sigma(I)$]	R_1 = 0.0386	R_1 = 0.0480	R_1 = 0.0430
	wR_2 = 0.0782	wR_2 = 0.0967	wR_2 = 0.0883
R indices (all data)	R_1 = 0.0591	R_1 = 0.0689	R_1 = 0.0554
	wR_2 = 0.0850	wR_2 = 0.1042	wR_2 = 0.0944
Largest difference in peak and hole (e Å^{-3})	1.776 and −1.140	3.458 and −1.125	0.862 and −0.360

2.5. Crystallographic studies

Crystals were mounted on quartz fibres. X-ray data were collected on a Bruker AXS APEX system, using Mo Kα radiation, with the SMART suite of programs [13]. Data were processed and corrected for Lorentz and polarization effects with SAINT [14], and for absorption effects with the program SADABS [15]. Structural solution and refinement were carried out with the SHELXTL suite of programs [16]. The structures were solved by either direct methods or Patterson maps to locate the heavy atoms, followed by difference maps for the light, non-hydrogen atoms. Organic hydrogen atoms were placed in calculated positions. Crystal and refinement data are summarized in Table 2.

Acknowledgements

This work was supported by an A*STAR Grant (Research Grant No. 012 101 0035) and one of us (P.K.C.) thanks ICES for a Research Scholarship.

Appendix A. Supplementary material

CCDC 681100, 681101 and 681102 contain the supplementary crystallographic data for this paper. These data can be obtained free of charge from The Cambridge Crystallographic Data Centre via www.ccdc.cam.ac.uk/data_request/cif. Supplementary data associated with this article can be found, in the online version, at doi:10.1016/j.jorganchem.2008.04.040.

References

[1] J.-K. Shen, D.S. Tucker, F. Basolo, R.P. Hughes, J. Am. Chem. Soc. 115 (1993) 11312–11318.
[2] P.K. Chan, W.K. Leong, K.I. Krummel, M.V. Garland, Eur. J. Inorg. Chem. (2006) 1568–1572.
[3] (a) M. Cheong, R. Schmid, T. Ziegler, Organometallics 19 (2000) 1973–1982;
(b) L. Gonsalvi, H. Adams, G.J. Sunley, E. Ditzel, A. Haynes, J. Am. Chem. Soc. 121 (1999) 11233–11234;
(c) D. Monti, G. Frachey, M. Bassetti, A. Haynes, G.J. Sunley, P.M. Maitlis, A. Cantoni, G. Bocelli, Inorg. Chim. Acta 240 (1995) 485–493.
[4] R. Ditchfield, R.P. Hughes, D.S. Tucker, E.P. Bierwagen, J. Robbins, D.J. Robinson, J.A. Zakutansky, Organometallics 12 (1993) 2258–2267.
[5] D.L. Lichtenberger, M.L. Hoppe, L. Subramanian, E.M. Kober, R.P. Hughes, J.L. Hubbard, D.S. Tucker, Organometallics 12 (1993) 2025–2031.
[6] E.W. Gowling, S.F.A. Kettle, Inorg. Chem. 3 (1963) 604–605.
[7] (a) R.P. Hughes, W. Kläui, J.W. Reisch, A. Müller, Organometallics 4 (1985) 1761–1766;
(b) W.A. Donaldson, R.P. Hughes, J. Am. Soc. 104 (1982) 4846–4859.
[8] M. Smith, J. March, March's Advanced Organic Chemistry: Reactions, Mechanisms and Structure, 5th ed., John Wiley & Sons, New York–Singapore, 2001.
[9] C. Lowe, V. Shklover, H. Berke, Organometallics 10 (1991) 3396–3399.
[10] (a) R.M. Tuggle, D.L. Weaver, J. Am. Chem. Soc. 92 (1970) 5523–5524;
(b) R.P. Hughes, J.M.J. Lambert, A.L. Rheingold, Organometallics 4 (1985) 2055–2057.
[11] R.P. Hughes, J.M.J. Lambert, D.W. Whitman, J.L. Hubbard, W.P. Henry, A.L. Rheingold, Organometallics 5 (1986) 789–797.
[12] L. Garlaschelli, R. della Pergola, S. Martinengo, Inorg. Synth. 28 (1989) 211–215.
[13] SMART Version 5.628, Bruker AXS Inc., Madison, WI, USA, 2001.
[14] SAINT+ Version 6.22a, Bruker AXS Inc., Madison, WI, USA, 2001.
[15] G.M. Sheldrick, SADABS, 1996.
[16] SHELXTL Version 5.1, Bruker AXS Inc., Madison, WI, USA, 1997.